

Effect of electric-field fluctuations on rotational revival amplitudes

Andrew J. Pearson and Thomas M. Antonsen

Institute for Research in Electronics and Applied Physics, University of Maryland, College Park, Maryland 20742, USA

(Received 30 April 2009; revised manuscript received 31 August 2009; published 12 November 2009)

We study numerically the behavior of rotational revivals in a molecular gas when subject to the fluctuating electric field of a background plasma. We model a molecule using a rigid rotor Hamiltonian and couple it to an electric field using permanent and induced multipole interaction terms. The evolution of the density matrix for the molecule is calculated for a short intense laser pulse, followed by a fluctuating background electric field. A broad superposition of angular momentum eigenstates of a molecule is created by the laser field, and the result of an ensemble average over initial molecular orientation is a set of recurring peaks in the probability density for observing a particular orientation—the so-called “rotational revivals.” The fluctuating background field is created using the dressed particle technique, and the result is a loss of coherence between the phases of the various basis states of the molecule, which causes a decreasing amplitude for subsequent alignment peaks. Modern short-pulse lasers operate with sufficient intensity to make this effect relevant to experiments in molecular alignment.

DOI: [10.1103/PhysRevA.80.053411](https://doi.org/10.1103/PhysRevA.80.053411)

PACS number(s): 37.10.Vz, 42.50.Wk

I. INTRODUCTION

There has been intense study of laser-induced molecular alignment in recent years, because of the availability of relatively small high-power short-pulse lasers [1]. Of relevance here is nonadiabatic alignment due to a laser pulse of duration much less than the inverse of the frequency associated with the first excited rotational state of the molecule [2,3]. This excites a broad superposition of phase-coherent angular momentum states that constitute the molecular wave function. Because of the energy dependence of the basis states of a rigid rotor, the phase alignment of the molecular wave function is periodic in time. The result is a series of sharp peaks in the probability density for observing a molecule with a particular orientation [4]. These peaks are referred to as “rotational revivals.” Experimentally, this effect can be observed by measuring the variation in the refractive index of the gas [5], or by Coulomb explosion imaging [6].

In an ideal system, the rotational revivals would continue indefinitely, however, in real systems, dissipative effects cause a loss of coherence between the phases of the various basis states [7], and so the amplitudes of successive revival peaks reduce until the revival structure disappears. A major contribution to this dissipation comes from molecular collisions [8]. In this paper, we investigate an additional mechanism for the disappearance of the revival structure, involving the electric field of a background plasma and its coupling to the various multipole moments of the molecules.

The paper is organized as follows: in Sec. II, we consider the different parameters involved in our system, and provide some justifying remarks to establish the relevance of the effect under consideration. In Sec. III, we discuss briefly the time evolution of the density matrix elements under the effect of the laser pulse, and then consider the modification of the multipole interaction terms due to a background plasma. In Sec. IV, we discuss the numerical techniques used, present the results of the numerical simulations for a variety of system parameters, and compare the results to scaling laws produced by a toy model. We conclude with a brief outlook.

II. DECOHERENCE DUE TO ELECTRIC FIELD FLUCTUATIONS

We first establish the conditions of relevance of the proposed effect. Specifically, we wish to show that the effect is observable for a reasonable choice of plasma parameters. As previously noted, the recurrence peaks occur because of a periodic phase alignment of the time evolution factors in the wave function, and so it is reasonable to suppose that the decoherence occurs because of a time-dependent alteration of the phase factor by the background field. To estimate the decay time, we take the form of the energy level shift from perturbation theory and define the decay time to be the time at which the phase shift is of order unity. Specifically, we estimate the decay time to be

$$\tau \sim \frac{\hbar}{\Delta E}, \quad (1)$$

where $\Delta E = \mu^2 E_l^2 / B$ is a typical second order change in the energy levels due to the field fluctuations, and $E_l = e / r_l^2$ is a typical fluctuating field strength. In these expressions, B is the rotational constant of the molecule, r_l is the typical distance between a molecule and an ion, and μ is the permanent dipole moment. The expression contains a second order term in the interaction strength because the linear term vanishes due to symmetry.

For the decay time due to collisional decoherence, we consider the measurements made by Chen *et al.* [5] for a number of different molecular gases at different pressures. These measurements give collisional decay times of 10–25 ps for pressures in the range 2–7 atmospheres. Substituting these numbers into the decay time equation suggests that for the effect under consideration to be observable in the presence of collisional decoherence, we must consider plasma densities of at least 10^{18} cm^{-3} . Since it is possible to completely ionize higher density gas samples with a laser pulse (for example, [9]), then it is possible to achieve such a plasma density while retaining sufficient neutral molecules, either through careful control of the laser intensity, or through the

use of an appropriately chosen mixture of gases.

The other important parameter to consider is the plasma temperature. In estimating the decay time in the manner shown above, we have assumed that the charged particles that interact with the molecule are essentially stationary. This is a reasonable assumption for a sufficiently cold molecular gas, since the ionizing laser pulse will be sufficiently short that the ion temperature will not be appreciably different from the neutral temperature. Conversely, the electrons will undergo heating through various mechanisms, for example, above threshold ionization and Raman scattering [10]. The resulting electron temperatures vary from 1 eV to 1 keV, and since the characteristic interaction time between an electron and a molecule will be much shorter than rotational frequency of the molecule, the electrons will only affect the decay time in the context of Debye shielding.

We conclude from these heuristic investigations that it is quite possible to observe this effect in an appropriately designed experiment. One may imagine a molecular gas that is partially ionized to create a plasma of the correct density and temperature, by choosing the pulse length, intensity, gas temperature, and gas mixture appropriately. If this plasma is left a sufficiently long time, then any rotational revivals will decay due to collisional decoherence and the electron plasma will have time to thermalize. A second laser pulse (presumably weaker, so as not to change the state of ionization) may then be introduced, and will generate another set of coherences. The effects of the background plasma on these coherences may then be measured.

III. CALCULATION OF DENSITY MATRIX ELEMENTS

In this paper, we consider a linear molecule, modeled as a modified rigid rotor interacting with an electric field through permanent dipole, induced dipole, and permanent quadrupole interactions. In the basis of eigenstates of the field-free Hamiltonian, the evolution of the density matrix is governed by

$$\frac{d}{dt}\rho_{IJ} = -i\omega_{IJ}\rho_{IJ} + \frac{i}{\hbar} \sum_K (\rho_{IK}V_{KJ} - V_{IK}\rho_{KJ}), \quad (2)$$

where V_{IJ} is an interaction matrix element and ω_{IJ} represents the difference in the unperturbed frequencies of states I and J and is given by

$$\omega_{IJ} = \frac{B}{\hbar}[i(i+1) - j(j+1)] - \frac{D}{\hbar}[i^2(i+1)^2 - j^2(j+1)^2]. \quad (3)$$

Here, $I=(i,m)$ and $J=(j,n)$ are double indices consisting of the total and directional angular momentum quantum numbers, B is the rotational constant of the molecule, and D is the centrifugal distortion constant for the molecule in its lowest vibrational state.

The most general interaction operator we consider takes the form

$$V_{IJ} = -\langle I|\boldsymbol{\mu} \cdot \mathbf{E} + \frac{1}{2}\mathbf{E} \cdot \underline{\boldsymbol{\alpha}} \cdot \mathbf{E} + \frac{1}{6}\underline{\mathbf{Q}}:\nabla\mathbf{E}|J\rangle, \quad (4)$$

where $\boldsymbol{\mu}$ is the permanent dipole moment, $\underline{\boldsymbol{\alpha}} \cdot \mathbf{E}$ is the induced dipole moment and $\underline{\mathbf{Q}}$ is the permanent quadrupole moment tensor.

We consider two types of electric field here. The first is the electric field of a laser pulse, which can be used to create a revival structure in a molecular gas. We are interested in pulse lengths that are long compared to the optical period, but short compared to the typical rotational time scale of a small diatomic molecule (on the order of picoseconds). This places us in the regime of nonadiabatic molecular alignment. By choosing a laser field for which there are many cycles over the duration of the pulse, we allow the cycle-averaging of the interaction terms in the Hamiltonian. A consequence of this is that interaction terms with odd powers in the field strength are negligible compared to those with even powers. We therefore consider only the induced dipole term for the laser pulse.

In the body-fixed frame of a molecule with the molecular axis chosen as the z axis, the polarizability tensor may be written as a diagonal matrix with entries α_{xx} , α_{yy} , and α_{zz} . In a coordinate system in which the molecular axis is defined by a unit vector $\hat{\mathbf{n}}$, the polarizability tensor takes the form

$$\underline{\boldsymbol{\alpha}} = \alpha_{\perp}\mathbf{1} + \Delta\alpha\hat{\mathbf{n}}\hat{\mathbf{n}}, \quad (5)$$

where $\alpha_{\perp} = \alpha_{xx} = \alpha_{yy}$ and $\Delta\alpha = \alpha_{zz} - \alpha_{\perp}$. We may choose the z axis as the direction with which to measure a component of angular momentum, and we may further choose the laser field to be polarized in this direction. Writing the laser field as

$$\mathbf{E}(t) = \text{Re}\{\hat{\mathbf{z}}E_0(t)\exp(-i\omega t)\}, \quad (6)$$

the interaction term for the laser is now

$$V_{IJ}^{(L)} = -\frac{1}{4}E_0^2(\alpha_{\perp}\delta_{IJ} + \Delta\alpha\langle I|\cos^2\theta|J\rangle). \quad (7)$$

Here, we have written $\cos\theta = \hat{\mathbf{n}} \cdot \hat{\mathbf{z}}$. The second term in Eq. (7) may be calculated using spherical harmonics.

The evolution of the density matrix elements for the molecule subjected to a laser pulse may now be found using either perturbation theory or numerical techniques. Having found them, we must find a measure of the alignment of a molecule in the gas. In the density matrix formalism, this measure is

$$[\cos^2\theta] = \sum_{I,J} \rho_{IJ}\langle J|\cos^2\theta|I\rangle, \quad (8)$$

where the square brackets denote the ensemble average over the angular momentum states.

The other type of electric field considered is the fluctuating background field due to the presence of a plasma. Unlike the laser field, we cannot choose to align the electric field vector and the angular momentum measurement axis, and so the interaction terms have an angular dependence of greater complexity. If we define the function

$$W = \hat{\mathbf{n}} \cdot \mathbf{E} = (\hat{\mathbf{n}} \cdot \hat{\mathbf{x}})E_x + (\hat{\mathbf{n}} \cdot \hat{\mathbf{y}})E_y + (\hat{\mathbf{n}} \cdot \hat{\mathbf{z}})E_z, \quad (9)$$

then the method for evaluating the matrix elements of W becomes clear. The interaction terms for each type of multipole coupling are given by

$$V_{IJ}^{(p)} = -|\boldsymbol{\mu}| \langle I|W|J \rangle \quad (10)$$

$$V_{IJ}^{(Q)} = -\frac{1}{6}(Q_{\perp} \nabla \cdot \mathbf{E} \delta_{IJ} + \Delta Q \langle I|\hat{\mathbf{n}} \cdot \nabla W|J \rangle) \quad (11)$$

$$V_{IJ}^{(I)} = -\frac{1}{2}(\alpha_{\perp} |E|^2 \delta_{IJ} + \Delta \alpha \langle I|W^2|J \rangle), \quad (12)$$

where we have written the quadrupole tensor in analogy to Eq. (5).

We wish to study the effect of this field on the revival structure created by the laser pulse. If the fluctuations are small and frequent, then an approximate analytic solution is possible, and the density matrix changes in proportion to the correlation function of the interaction at two different times. For the system parameters of interest, however, the fluctuations are large and infrequent, and so we resort to a numerical solution.

We proceed by modeling the plasma as a collection of dressed particles [11]. In this method, we consider a test particle moving in a straight line through a plasma at some velocity \mathbf{v} . Such a particle will acquire a shielding cloud from the plasma, and this will alter its potential. For a test particle at rest, this is the familiar Debye shielding effect, but for a moving particle the shielding is modified in an anisotropic way. We refer to the combination of the test particle and its shielding cloud as a dressed particle.

Allowing for transient effects to vanish, the potential of a test particle is given by

$$\phi(\mathbf{x}_{ob}, \mathbf{x}, \mathbf{v}, t) = 4\pi q \int \frac{d^3k}{(2\pi)^3} \frac{\exp[i\mathbf{k} \cdot (\mathbf{x}_{ob} - \mathbf{x} - \mathbf{v}t)]}{k^2 D(\mathbf{k}, \mathbf{k} \cdot \mathbf{v})}, \quad (13)$$

where \mathbf{x} is the initial position of the dressed particle and \mathbf{x}_{ob} is the point of observation of the potential [12]. $D(\mathbf{k}, \mathbf{k} \cdot \mathbf{v})$ is the dielectric function of the plasma, given by

$$D(\mathbf{k}, \mathbf{k} \cdot \mathbf{v}) = 1 - \sum_{\alpha} \frac{\omega_{p\alpha}^2}{k^2} \int \frac{d^3v'}{(2\pi)^3} \frac{\mathbf{k} \cdot \nabla_{\mathbf{v}'} f_{0\alpha}}{\mathbf{k} \cdot (\mathbf{v}' - \mathbf{v}) - i0^+}, \quad (14)$$

where α refers to the plasma species and $f_{0\alpha}$ is the unperturbed plasma distribution function.

We note that in the current approach, we take the test particle velocities to be constant and unaffected by the molecule's electric field. The result is that over time, there will be continuous energy transfer from the plasma particles to the molecule. In reality, the energy gain of the molecule is limited, and the molecule will come into thermal equilibrium with the plasma. We assume that this process occurs over a longer period of time than the destruction of the recurrences.

The plasma will be created by the partial ionization of the molecular gas by the laser pulse. Since this is very short, we

expect the molecular ions to be thermally distributed at the same temperature as the unionized molecules. The electrons will, in general, be much faster than the ions. We therefore use a dressed particle model with molecule-mass test particles, shielded by fast electrons and stationary ions. We choose to exclude electrons as test particles because we expect the ions to remain in proximity to a molecule for much longer than the electrons, and so the ions will have the dominant effect. In this case, we are interested in the low speed approximation for the potential. This calculation may be found in Ref. [13], and the result is

$$\phi(\mathbf{r}, \mathbf{v}) \approx \frac{q}{r} \left[\exp(-rk_D) + \frac{v}{u_{th}} g(r, \hat{\mathbf{r}} \cdot \hat{\mathbf{v}}) + \dots \right], \quad (15)$$

where $\mathbf{r} = \mathbf{x}_{ob} - \mathbf{x} - \mathbf{v}t$, v (u) is a velocity associated with ions (electrons), and k_D is the reciprocal of the Debye length. The function $g(r, \mathbf{r} \cdot \mathbf{v})$ is given by

$$g(r, \hat{\mathbf{r}} \cdot \hat{\mathbf{v}}) = \frac{1}{\sqrt{2\pi}} (\hat{\mathbf{r}} \cdot \hat{\mathbf{v}}) \left[\frac{rk_D}{2} \left(1 - \frac{1}{rk_D} + \frac{1}{(rk_D)^2} \right) \exp(rk_D) E_1(rk_D) + \frac{rk_D}{2} \left(1 + \frac{1}{rk_D} + \frac{1}{(rk_D)^2} \right) \exp(-rk_D) \text{Ei}(rk_D) - 1 \right], \quad (16)$$

where E_1 and Ei are exponential integral functions.

Once we calculate the electric field for a collection of test particles, we may compute the density matrix and thus the ensemble average molecular alignment over the various rotational states available, as per Eq. (8). We then repeat this procedure for a number of different test particle configurations to generate an ensemble average of the molecular alignment over each molecule in the gas.

IV. NUMERICAL SIMULATION RESULTS

In this section, we present the results of the numerical simulations. As previously stated, the goal is to calculate the time-dependent expectation value $[\cos^2 \theta]$ for a fluctuating background field. We simulate the background field by calculating the electric field components at the center of a spherical region containing a number of test particles. These test particles move in straight lines from random initial positions and with random velocities, all generated from the appropriate distribution functions. Test particles that leave this region are replaced by re-generating their initial conditions to place them somewhere on the system boundary with an ingoing velocity. The number of test particles present in the system at any one time is chosen to correspond to a certain plasma density.

To calculate the density matrix, we use the Cash-Karp embedded Runge-Kutta method [14]. This allows for an efficient adaptive stepsize calculation. We begin with a thermal distribution of rotational states, and calculate the effect of the laser pulse strike on the density matrix. We will consider a laser beam with an intensity of 10^{12} W/cm², which is large enough to create a revival structure while avoiding compli-

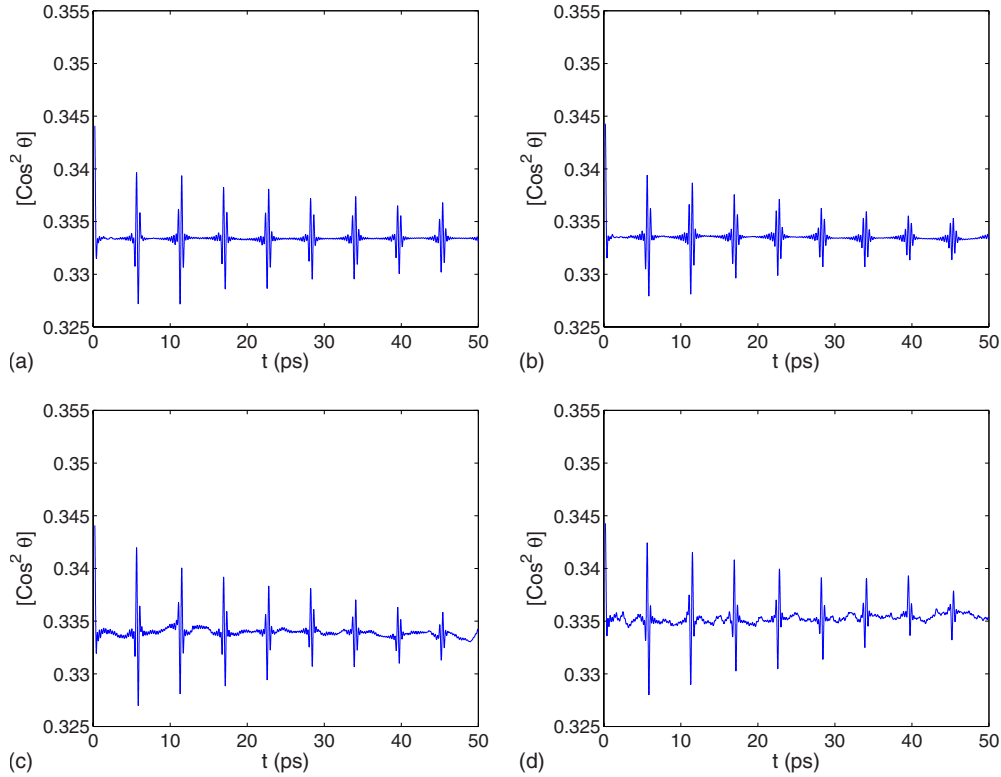


FIG. 1. (Color online) Average alignment of HCN molecules vs time for (a) the permanent dipole interaction with $n=10^{18} \text{ cm}^{-3}$ and $T_e=1 \text{ eV}$, (b) the permanent dipole interaction with $n=10^{18} \text{ cm}^{-3}$ and $T_e=10 \text{ eV}$, (c) the permanent quadrupole interaction with $n=10^{19} \text{ cm}^{-3}$ and $T_e=1 \text{ eV}$, and (d) the induced dipole interaction with $n=10^{20} \text{ cm}^{-3}$ and $T_e=1 \text{ eV}$.

cations introduced when the populations of the angular momentum states change significantly. This intensity is not sufficient to cause the appropriate level of ionization, and so our simulations correspond to an experiment of the type described in Sec. II. We choose the pulse length to be 100 fs and the optical frequency to be 10^{15} Hz , both typical of a short-pulse laser. This optical frequency will be sufficiently large compared to the characteristic molecule rotational frequency as to allow the cycle averaging discussed in the derivation of Eq. (7).

The density matrix calculated for the laser strike is then used as an initial condition for the calculation of the evolution of the density matrix with the fluctuating background field present. We use this to calculate the amount of alignment of a single molecule in the gas, and then repeat this procedure for a large number of test particle configurations, so as to obtain an average over many molecules.

In these simulations, we will consider the molecules Hydrogen Cyanide (HCN) and Nitrogen (N_2). HCN is an example of a linear molecule with a strong permanent dipole moment, while N_2 is a common dipole. We will consider the different multipole interactions separately, since we expect their sizes to differ significantly from one another. This may be seen by estimating in each case the size of the interaction term for a Coulomb field at distance $n^{-1/3}$. The free parameters in these simulations are the electron and ion temperatures, and the plasma density.

The first set of results is for HCN with the background ions at room temperature. The parameters for HCN associated with the molecular dynamics are $B=1.48 \text{ cm}^{-1}$ and D

$=3.33 \times 10^{-6} \text{ cm}^{-1}$, and multipole moments are $|\mu|=2.96 \times 10^{-18} \text{ esu cm}$ [15], $\Delta Q=7.68 \times 10^{-26} \text{ esu cm}^2$, and $\Delta\alpha=2.0 \times 10^{-24} \text{ cm}^3$ [16]. We considered electron temperatures of 1 and 10 eV, and for the permanent dipole case, we chose a plasma density of 10^{18} cm^{-3} . For higher order moments, we chose higher densities, since we expect the decay time to be longer. This choice reduces computation time and avoids large-time effects associated the centrifugal stretching.

Figure 1 demonstrates the revival structure and the decay. Here, the letters P , Q , and I indicate the different multipole interactions considered. Specifically in Figs. 1(a) and 1(b) only the permanent dipole interaction is allowed, in Fig. 1(c) only the permanent quadrupole interaction is allowed, and in Fig. 1(d), only the induced dipole interaction is allowed. As the permanent dipole interaction is strongest, followed by the quadrupole and induced dipole interaction, decoherence appears at relatively lower densities in Figs. 1(a) and 1(b), followed by successively higher densities in Figs. 1(c) and 1(d). To understand the revival structure, we consider the form of the average alignment, as seen in Eq. (8). This may be rewritten

$$[\cos^2 \theta] = \sum_{I,J} \alpha_{IJ} \exp(-i\omega_{IJ}t) \langle J | \cos^2 \theta | I \rangle, \quad (17)$$

where $\alpha_{IJ} = \rho_{IJ} \exp(i\omega_{IJ}t)$. In field-free conditions, α_{IJ} is a constant, and revival peaks occur because the phase factors in Eq. (17) align periodically. Comparing Eqs. (3) and (17), the revival period is seen to be $\tau = \pi\hbar/B$. For HCN, the revival period is calculated to be $\tau=11.3 \text{ ps}$, which is consis-

tent with our results. At the halfway point between revival peaks, there exist sharp decreases in the alignment. This is because at half revival times, half of the complex exponentials in Eq. (17) are phase aligned with value 1 and the other half are aligned with value -1 . The terms in the sum thus interfere destructively leading to a decrease in the alignment.

There is a second set of peaks due to the second term in Eq. (3). Because the constant D is much smaller than B , however, these peaks are much wider than the revival peaks, and their recurrence period is much larger. If we were to observe a revival structure in the absence of decoherence for a sufficiently long time, we would observe the revival peaks reducing in size until they vanish, and then periodically reappear at times $\tau_D = \pi\hbar/D$ (This is the long-time centrifugal effect alluded to earlier). We tend not to observe this effect, since there is always sufficient decoherence to destroy the revival structure before time τ_D .

In the presence of a background plasma, the coefficients α_{IJ} are no longer constant, but are time-dependent complex functions. For each set of test particles, the complex exponential part of each term in the sum in Eq. (17) is modified by the phase of the coefficient. If the phase change in the coefficient is small between the laser strike and the first revival time, then the amplitude of each revival peak is reduced. At later times, the phase change is greater than at earlier times, and so the revival peaks are destroyed completely. If the phase change becomes large on a time scale smaller than the recurrence time, then the revival structure is destroyed before the first peak appears.

The next set of results is for N_2 , again with the ions at room temperature. The molecular parameters for N_2 are $B = 1.99 \text{ cm}^{-1}$ and $D = 5.76 \times 10^{-6} \text{ cm}^{-1}$ [17]. The quadrupole moment for N_2 is $\Delta Q = 1.49 \times 10^{-26} \text{ esu cm}^2$ [16].

The graphs in Fig. 2 once more demonstrate the revival structure. We note that the decay time is much greater for N_2 than for HCN. This is because the quadrupole coupling constant for HCN is ~ 5 times greater than that for N_2 (note that we have suppressed the permanent dipole interaction for HCN, which is its dominant interaction), and so the background field is much more effective in exciting different rotational states of the molecules and disrupting the phase coherence of the revivals. In the N_2 graph, the additional peaks at $\tau/4$ and $3\tau/4$ are due to the requirement that the wave function of N_2 must be symmetric under exchange of the nuclei, since Nitrogen atoms are spin-1 bosons. This means, for example, that if the wave function for some rotational state is even, then only even two-nucleus wave functions are allowed. Since for combinations of two spin-1 particles there are six symmetric states and three antisymmetric states, the populations of even rotational states are weighted by a factor of two.

The final set of results consists of a detailed study of the decay time as a function of the ion thermal velocity and the plasma density. These results are obtained by generating alignment vs time graphs and fitting an exponential curve to the recurrence peaks. In Fig. 3(a), the decay times were obtained for a plasma density of 10^{18} cm^{-3} , while in Fig. 3(b), the results were obtained for ions with a thermal velocity corresponding to room temperature. In both cases, we considered only the permanent dipole interaction for HCN, and

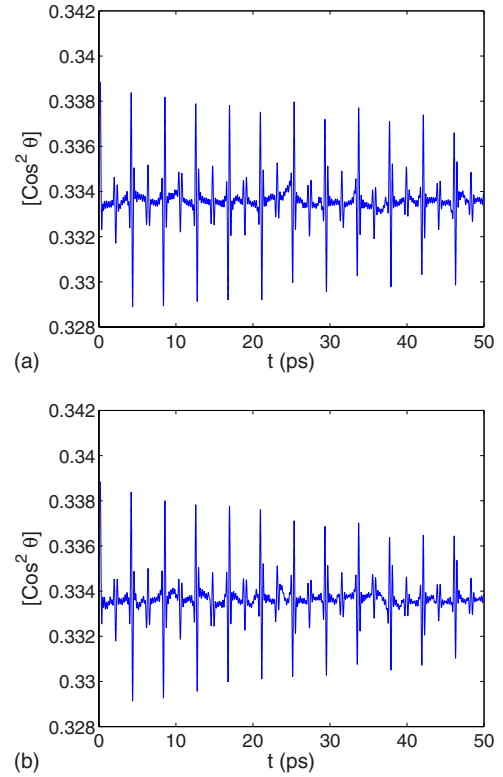


FIG. 2. (Color online) Average alignment of N_2 molecules vs time for (a) the quadrupole dipole interaction with $n = 10^{19} \text{ cm}^{-3}$ and $T_e = 1 \text{ eV}$, and (b) the quadrupole dipole interaction with $n = 10^{19} \text{ cm}^{-3}$ and $T_e = 10 \text{ eV}$.

the electron temperature was held constant at 1 eV.

We can explain these results by considering the quantum mechanical description of a single molecule subject to the electric field of a passing ion. To begin, we note that for a constant electric field, the energy of the state $|l, m\rangle$ shifts by an amount

$$\Delta E_{lm} = \sum_{|j,n\rangle \neq |l,m\rangle} \frac{|\langle l,m | \boldsymbol{\mu} \cdot \mathbf{E} | j,n \rangle|^2}{E_l - E_j} = \frac{\mu^2 E^2}{B} \Delta_{lm}. \quad (18)$$

This term can be calculated from second order in perturbation theory. The shift is second order because the diagonal matrix elements of the interaction vanish identically. In general, this term will depend on the orientation of the electric field and the particular eigenstate under consideration, but we neglect these and focus on scaling laws. The energy shift is important, since it is related to the phase change that destroys the alignment in the evolution terms in Eq. (17).

Decoherence will occur even if all ions are stationary due to the fact that each molecule experiences a different electric field depending on its proximity to neighboring ions. The typical electric field strength a molecule experiences is

$$E \approx \frac{e}{r_l^2}, \quad (19)$$

where $r_l = n^{-1/3}$ is the inter-ion spacing. The fluctuations in the electric field strength are comparable to this value. Thus, there will be variations in ΔE_{lm} . The functional form of the

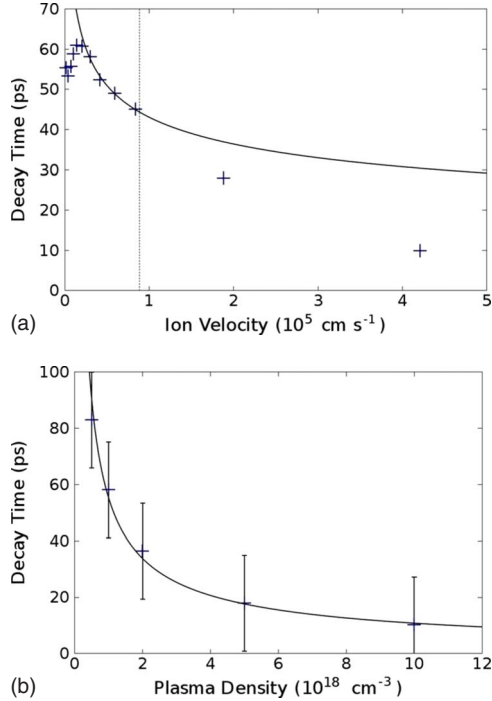


FIG. 3. (Color online) Dependence of the decay time of alignment of HCN on (a) ion thermal velocity at fixed density $n = 10^{18} \text{ cm}^{-3}$ and (b) density at fixed ion temperature $T_i = 0.025 \text{ eV}$.

decay in time is determined by the distribution of electric field values, and is probably not exponential. Since the fluctuations in electric field magnitude are as large as the typical value, we estimate that decoherence will occur in a time

$$\tau_s = \frac{\pi\hbar}{\Delta E_{lm}} = \frac{\pi\hbar B r_l^4}{\mu^2 e^2 \Delta_{lm}} \sim n^{-4/3}. \quad (20)$$

Averaging over the various field angles, and weighting by angular momentum state populations, we estimate the decay time to be 24 ps. This is not dissimilar to the first few data points in Fig. 3(a).

If the ions are moving, the decoherence time can be shorter than τ_s . This is because with time, an ion is likely to come much closer to a molecule than the typical ion spacing r_l . The strong electric field occurring during such an encounter gives a phase change much bigger than calculated for static ions. For this regime to be of interest, the static decoherence time must be much longer than the typical time it takes an ion to move a distance equal to the inter-ion spacing, i.e., $\tau \gg r_l/u_{th}$, where u_{th} is the typical ion velocity.

For the case of ions moving at a low speed such that their transit time (i.e., time spent in proximity to molecule) is large compared to the characteristic evolution time of the eigenstates, we may use the adiabatic approximation to estimate the phase change. Which states satisfy the adiabatic approximation will be discussed subsequently. For the moment, we assume that all do. Here, we assume that the ion moves in a straight line with velocity u and impact parameter b and causes a time-dependent energy shift

$$\Delta E \approx \frac{\mu^2 e^2}{B} \frac{1}{(b^2 + u^2 t^2)^2}. \quad (21)$$

The total phase shift in the molecular wave function caused by a single ion is then

$$\Delta\phi = \int dt \frac{\Delta E(t)}{\hbar} = \frac{\pi\mu^2 e^2}{2\hbar B} \frac{1}{b^3 u}. \quad (22)$$

If we now suppose that each phase shift happens instantaneously (which is equivalent to assuming that the decay time we will calculate is long compared to the ion transit time), and further assume that the phase shifts due to different ions are independent events, we can evaluate the rate of decoherence.

To do this, we break time into N intervals of duration $\Delta t = t/N$. We assume that during each time interval, there is a probability of a random phase change $\Delta\phi$ due to a close encounter with an ion. The net phase change to the wave function is the sum of all random phase changes. The average of the wave functions of an ensemble of molecules will evolve in time according to

$$\langle \exp(i \sum_{\Delta t} \Delta\phi) \rangle = \left[\int dP \exp(i\Delta\phi) \right]^N, \quad (23)$$

where dP is the probability of a phase change $\Delta\phi$ in the interval $d(\Delta\phi)$, and we have assumed that the phase changes in the N different time intervals are independent. As time $t = N\Delta t$ goes to infinity, the average phase factor will decay.

We evaluate this decay by assuming that the amount of decay in a single time interval is small. Thus, we write in the $N \rightarrow \infty$ limit

$$\begin{aligned} \langle \exp(i \sum_{\Delta t} \Delta\phi) \rangle &= \left\{ 1 + \frac{t}{N} \int \frac{dP}{\Delta t} [\exp(i\Delta\phi) - 1] \right\}^N \\ &\approx \exp(-\nu t), \end{aligned} \quad (24)$$

where

$$\nu = - \int \frac{dP}{\Delta t} [\exp(i\Delta\phi) - 1]. \quad (25)$$

We note the ν has both a real and an imaginary part. The real part controls the decay of the recurrences while the imaginary part describes the average energy shift. To evaluate the probability per unit time that there will be a phase change $\Delta\phi$, we note that in the time interval Δt , the number of ions with speed u in the range du entering a sphere of radius b surrounding the molecule is

$$dN = 4\pi b^2 n \frac{1}{\sqrt{2}u_{th}} \exp(-u^2/u_{th}^2) u du \Delta t. \quad (26)$$

All of these ions will have an impact parameter less than b . Thus, the number of ions with impact parameter b in the interval db passing per unit time is obtained by differentiating with respect to b

$$\frac{dP}{\Delta t} = \frac{dN db}{db \Delta t} = \frac{8\pi^{1/2}n}{u_{th}} u \exp(-u^2/u_{th}^2) du b db. \quad (27)$$

We may now substitute Eq. (22) for $\Delta\phi$, and change variables of integration to $\xi = u/u_{th}$ and $b = b_c\beta$, where

$$b_c^3 = \frac{\pi\mu^2 e^2}{2\hbar B u}, \quad (28)$$

to obtain for the decoherence time

$$\tau_d^{-1} = \nu = -nu_{th}^{1/3} \left(\frac{\pi\mu^2 e^2}{2\hbar B} \right)^{2/3} \Lambda, \quad (29)$$

where

$$\Lambda = 8\pi^{1/2} \int_0^\infty d\xi \xi^{1/3} \exp(-\xi^2) \int_0^\infty \beta d\beta [\exp(i/\beta^3) - 1]. \quad (30)$$

Numerical evaluation gives $\Lambda = -6.43 + 11.14i$. Comparing the static decoherence time τ_s given by Eq. (20) and the dynamic decoherence time τ_d given by Eq. (29), we note that $\tau_d^{-1} \sim \tau_s^{-2/3} (u_{th}/r_l)^{1/3}$. Since at the boundary separating the static and dynamic cases $u_{th} \sim r_l/\tau_s$, the two results are in agreement.

There is some evidence of the density and temperature dependences implied by Eq. (29) in Fig. 3. Figure 3(a) shows the dependence of the decoherence time on ion thermal velocity at fixed density. As the thermal velocity tends to zero, the decoherence time tends to a fixed value. As the thermal velocity is increased, the decoherence time decreases. The solid line in Fig. 3(a) shows the scaling expected from Eq. (29). The range over which this scaling applies is too small to say conclusively that it is observed.

The vertical dashed line indicates the velocity of an ion with a transit time corresponding to the period of the $l=1$ eigenstate. For larger ion velocities, we expect that some of the eigenstates that comprise the wave function will evolve too quickly, and the adiabatic approximation will break down. At lower ion velocities, the decay time is not constant as expected in the static approximation, but varies within a small range.

We expect the adiabatic result to apply for the density dependence of the decay time, as shown in Fig. 3(b). This is because the density dependent adiabatic boundary remains above the ion thermal velocity for all densities considered, and also because we know that the result for the case $n = 10^{18} \text{ cm}^{-3}$ is consistent with the adiabatic approximation. A direct fit of the data points reveals a power law dependence somewhat different than expected, however, the correct power law dependence will fit within the uncertainty of the result. This uncertainty is due to an ambiguity in the method used for calculating the decay time. The adiabatic approximation predicts a simple exponential decay of the revival peaks, and we assume this when using the peak heights of the revival graphs to predict the decay time. The decay is probably not this simple, and we quantify the difference between the exponential estimate of the decay and the true decay pattern by calculating exponential decay times from all possible peak pairs in Fig. 1(a). From these results, we see a variation in decay times of about 12 ps either side of the stated time.

V. CONCLUSION

In conclusion, we studied the effect of a fluctuating electric field on the coherence of a set of rotational revivals in a molecular gas. For significant ionization fractions, we found that the decay time for the revival amplitudes was on the order of picoseconds to tens of picoseconds. The permanent dipole was shown to be the most effective coupling for decoherence, followed by the quadrupole moment. We did not explore the induced dipole case because of limited computing resources, but from the scaling it appears that the quadrupole term will always dominate. Finally, for the parameters investigated the decoherence process is complex involving interplay between the ion motion and the break down of adiabaticity of the rotational states. In this regime computation is necessary to arrive at a quantitative value of the decoherence time.

ACKNOWLEDGMENT

This work was supported by the U.S. Department of Energy.

-
- [1] Henrik Stapelfeldt and Tamar Seideman, *Rev. Mod. Phys.* **75**, 543 (2003).
 [2] Tamar Seideman, *J. Chem. Phys.* **103**, 7887 (1995).
 [3] Claude M. Dion, Arne Keller, Osman Atabek, and André D. Bandrauk, *Phys. Rev. A* **59**, 1382 (1999).
 [4] Tamar Seideman, *Phys. Rev. Lett.* **83**, 4971 (1999).
 [5] Y.-H. Chen, S. Varma, A. York, and H. M. Milchberg, *Opt. Express* **15**, 11341 (2007).
 [6] P. W. Dooley, I. V. Litvinyuk, Kevin F. Lee, D. M. Rayner, M. Spanner, D. M. Villeneuve, and P. B. Corkum, *Phys. Rev. A* **68**, 023406 (2003).
 [7] S. Ramakrishna and Tamar Seideman, *Phys. Rev. Lett.* **95**, 113001, (2005).
 [8] S. Ramakrishna and Tamar Seideman, *J. Chem. Phys.* **124**, 034101, (2006).
 [9] W. J. Blyth, S. G. Preston, A. A. Offenberger, M. H. Key, J. S. Wark, Z. Najmudin, A. Modena, A. Djaoui, and A. E. Dangor, *Phys. Rev. Lett.* **74**, 554 (1995).
 [10] A. A. Offenberger, W. Blyth, E. Dangor, A. Djaoui, M. H. Key, Z. Najmudin, and J. S. Wark, *Phys. Rev. Lett.* **71**, 3983 (1993).
 [11] N. Rostoker, *Nucl. Fusion* **1**, 101 (1961).
 [12] Nicholas A. Krall and Alvin W. Trivelpiece, *Principles of Plasma Physics* (McGraw-Hill, New York, 1973).

- [13] Gilbert Cooper, *Phys. Fluids* **12**, 2707 (1969).
- [14] J. R. Cash and Alan H. Karp, *ACM Trans. Math. Softw.* **16**, 201 (1990).
- [15] C. H. Townes and A. L. Schawlow, *Microwave Spectroscopy* (McGraw-Hill, New York, 1955).
- [16] J. O. Hirschfelder, C. F. Curtiss, and R. B. Bird, *Molecular Theory of Gases and Liquids* (Wiley, New York, 1954).
- [17] G. Herzberg, *Molecular Spectra and Molecular Structure: Spectra of Diatomic Molecules*, 2nd ed. (Krieger Malabar, FL, 1989), Vol. I.